

# Van Hove singularities in stabilizer entropy densities

Daniele Iannotti<sup>1,2,\*</sup>, Lorenzo Campos Venuti<sup>2,3</sup> and Alioscia Hamma<sup>1,2,3</sup>

<sup>1</sup>Scuola Superiore Meridionale, Largo S. Marcellino 10, 80138 Napoli, Italy <sup>2</sup>Istituto Nazionale di Fisica Nucleare (INFN) Sezione di Napoli, Napoli, Italy <sup>3</sup>Università degli Studi di Napoli Federico II, Dipartimento di Fisica Ettore Pancini, Napoli, Italy

**E-mail:** \* d.iannotti@ssmeridionale.it

**Keywords:** Haar measure, Stabilizer Rényi entropies, Van Hove singularities, Incompatibility

---

## Abstract

The probability distribution of a measure of non-stabilizerness, also known as magic, is investigated for Haar-random pure quantum states. Focusing on the stabilizer Rényi entropies, the associated probability density functions (PDFs) are found to display distinct non-analytic features analogous to Van Hove singularities in condensed matter systems. For a single qubit, the stabilizer purity exhibits a logarithmic divergence at a critical value corresponding to a saddle point on the Bloch sphere. This divergence occurs at the  $|H\rangle$ -magic states, which hence can be identified as states for which the density of non-stabilizerness in the Hilbert space is infinite. An exact expression for the PDF is derived for the case  $\alpha = 2$ , with analytical predictions confirmed by numerical simulations. The logarithmic divergence disappears for dimensions  $d \geq 3$ , in agreement with the behavior of ordinary Van Hove singularities on flat manifolds. In addition, it is shown that, for qubits systems, the linear stabilizer entropy is directly related to the *partial incompatibility* of quantum measurements, one of the defining properties of quantum mechanics, at the basis of Stern-Gerlach experiments.

---

## 1 Introduction

Characterizing features of quantum resources [1–3] has been an important and challenging issue since the development of quantum computation in the past years, beyond, of course, the fundamental reasons connected to understand quantum mechanics. In this context, entanglement played an enormous role as its power for quantum algorithms was made clearer, as well as being able to distinguish quantum mechanics from classical theories [4, 5]. Over the past twenty years, another important resource, non-stabilizerness, or *magic*, has taken shape, rooted in the pioneering work of Bravyi and Kitaev [6]. They demonstrated that non-Clifford gates, essential for universal quantum computation, can be realized by augmenting stabilizer operations (i.e., Clifford gates and projective measurements) with special nonstabilizer, or “magic” states. The fundamental insight is that while stabilizer operations can typically be implemented in a fault-tolerant manner, often via transversal methods in quantum error-correcting codes [7], non-Clifford gates remain considerably more challenging to protect against noise [8, 9]. Additionally, magic plays an important role in understanding the classical simulability of quantum circuits. Namely, circuits consisting only of stabilizer operations can be efficiently simulated on a classical computer [10], whereas allowing for the presence of nonstabilizer states drastically increases the simulation complexity [11].

The interest in understanding the main features of magic [2, 12–21] has grown rapidly, since its first insights. Spanning from quantum circuit [22–31], condensed matter and many-body physics [32–61], to nuclear physics [62–64], particle physics and lattice gauge theories [65–71], even conformal field theories [72–75] and Bell’s inequalities [76, 77], this body of work both analytical and numerical was accelerated by the introduction of a new magic monotone, the *Stabilizer Rényi entropy* (SRE) [78].

Thus, SRE provides a unifying language to quantify how far a quantum state departs from the stabilizer polytope, capturing the essential quantumness required for universal computation. Yet, despite the extensive use of these quantities in both theoretical and experimental settings, much less is known about their statistical properties when quantum states are drawn uniformly from the Hilbert space according to the Haar measure.

In this work, we study the Haar-induced probability densities of stabilizer purities and their corresponding entropies. The problem of describing these probability density functions (PDFs) in the case of magic is related to the interesting mathematical question of characterizing the intersection between an  $\ell_2$  and an  $\ell_{2\alpha}$  sphere. We show that, even for the simplest case of a single qubit, these distributions encode rich geometric information. By mapping the problem to the density of states of a fictitious energy function defined on the Bloch sphere, we uncover the emergence of Van Hove singularities/logarithmic divergencies characteristic of two-dimensional dispersions at saddle points of the energy surface, as already noted in [79]. In the case of one qubit we find that the logarithmic divergencies in the PDFs take place at the so-called magic states  $|H\rangle$ , defined first in the original work of Bravyi and Kitaev [6] (see Fig. 1). In a sense this

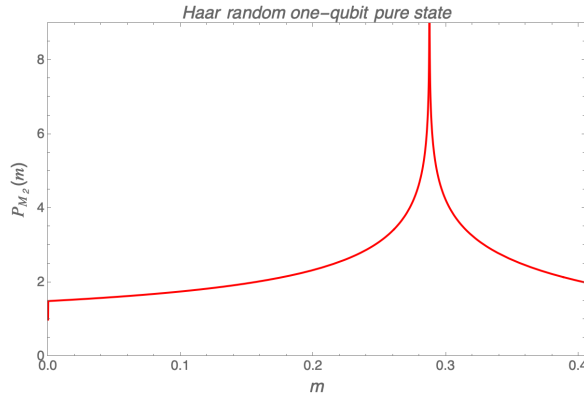


Figure 1: Probability density function,  $P_{M_2}(m)$ , of the random variable SRE of order two,  $m = M_2(|\psi\rangle)$  (see Eq. (2)), according to the Haar measure for one qubit. The support of  $P_{M_2}$  is the interval  $[0, \ln(3/2) = 0.405\dots]$ . The divergence, of logarithmic type, takes place at  $m_c = \ln(4/3) = 0.287\dots$ , corresponding to the 12 magic states in the Clifford orbit of  $|H\rangle = (|0\rangle + e^{i\pi/4}|1\rangle)/\sqrt{2}$ .

shows that  $|H\rangle$ -states are more resilient (in a statistical sense) because there is a large number of magic states with similar value of non-stabilizerness. We provide explicit analytical results for the stabilizer entropy and purity with Rényi index  $\alpha = 2$ , numerically validate the predicted logarithmic divergence, and discuss the absence of such singularities in higher-dimensional Hilbert spaces. Borrowing results for the density of states in solids, one may be led to conclude that van Hove singularities in  $d = 2$  are present in the probability density of any quantity defined on the Bloch sphere. One subtlety to remember is that the probability densities considered here are defined on a curved base manifold, the (Bloch) sphere, as opposed to a flat manifold, as is the standard case for the density of states in solids. Indeed, we find that other physically interesting quantities defined on the Bloch sphere, such as coherence or mean energy, do not display logarithmic divergence in their PDFs. So far, non-stabilizerness as measured by SRE (and likely also by the magic trace distance see the discussion in Sec. 7 [80]), are the only cases where this logarithmic divergencies are observed. Finally, we show how stabilizer purities, beside having a clear information-theoretic [78] and operational [81] interpretation, have a direct meaning in terms of fundamental quantum mechanics concepts, namely *partial incompatibility* of observables and bases.

## 2 Measures of non-stabilizerness

Throughout the paper, we consider  $\psi = |\psi\rangle\langle\psi|$  to be a pure state on the Hilbert space  $\mathcal{H}$  of  $L$  qubits of dimension  $d = 2^L$ . Acting on  $\mathcal{H}$ , there is a natural and preferential operator basis given by Pauli operators  $P \in \mathbb{P}_L$ , i.e.  $n$ -fold tensor products of ordinary Pauli matrices  $\mathbb{1}, X, Y, Z$ . The subgroup of unitary matrices that maps Pauli operators to Pauli operators is called the Clifford group, denoted as  $\mathcal{C}_L$  [82, 83]. The set of *pure stabilizer states* of  $\mathcal{H}$  is defined as the orbit of the Clifford group through the computational basis states  $|i\rangle$  (the eigenstates of the  $Z$  operator) [84]:

$$\text{PSTAB} := \{C|i\rangle, C \in \mathcal{C}_L\}. \quad (1)$$

Equivalently, a pure stabilizer state can be defined as the common eigenstate of  $d$  mutually commuting Pauli strings.

Roughly speaking, a quantum circuit that only produces stabilizer states can be efficiently simulated by a classical computer. More precisely, the *Gottesman-Knill theorem* [10] states that any quantum process that can be represented by an initial stabilizer state upon which one performs i) Clifford unitaries; ii) measurements of Pauli operators; and iii) Clifford operations conditioned on classical randomness; can be simulated by a classical computer in polynomial time. Since the set of stabilizer states is by definition closed under Clifford operations, some resources, such as unitary operations outside the Clifford group or states not in PSTAB, need to be injected in the system in order to allow for universal quantum computation. These non-stabilizer resources, referred to as *non-stabilizerness* (or *magic*) of the state, have been proven to be a useful resource for universal quantum computation [6] and several measures have been proposed to quantify them [12, 85]. Here we will focus on the essentially only computable measure for non-stabilizerness, namely the *Stabilizer Rényi Entropy* (SRE) [78]:

**Definition 1** (Stabilizer entropies [78]). *Let  $|\psi\rangle$  be a pure quantum state and  $\mathbb{R} \ni \alpha \geq 2$ . The  $\alpha$ -stabilizer Rényi entropy (SRE) is defined as*

$$M_\alpha(|\psi\rangle) := \frac{1}{1-\alpha} \ln \Xi_\alpha(|\psi\rangle), \quad (2)$$

where  $\Xi_\alpha$ 's are the stabilizer purities (SP)<sup>1</sup>

$$\Xi_\alpha(|\psi\rangle) := \frac{1}{d} \sum_{P \in \mathbb{P}_L} |\langle \psi | P | \psi \rangle|^{2\alpha}. \quad (3)$$

Another useful quantifier of non-stabilizerness, analogous to the linear entropy of entanglement, is given by the linear stabilizer entropy defined as [87]:

$$M_\alpha^{\text{lin}}(\psi) := 1 - \Xi_\alpha(\psi). \quad (4)$$

Both of these measures are: i) faithful, i.e.  $M_\alpha(\psi) = M_\alpha^{\text{lin}}(\psi) = 0 \Leftrightarrow \psi \in \text{PSTAB}$ ; ii) non-increasing under free operations, that is, operations that send states in PSTAB to states in PSTAB; and iii) additive under tensor product, namely  $M_\alpha(\psi \otimes \sigma) = M_\alpha(\psi) + M_\alpha(\sigma)$ , or multiplicative for the stabilizer purity  $\Xi_\alpha$ , i.e.  $\Xi_\alpha(\psi \otimes \sigma) = \Xi_\alpha(\psi) \Xi_\alpha(\sigma)$ .

Both linear and SREs are regarded as good monotones for the pure-state resource theory of stabilizer computation [88] and have a clear operational meaning [87], hence numerous schemes have been proposed to study them experimentally [89–93]. In recent years, SREs have emerged as a powerful diagnostic of diverse quantum phenomena. They capture features of error correction [94] and measurement-induced phase transitions [95, 96], and are closely connected to property testing protocols [81, 97]. SREs are further related to participation entropy [98], which provides insight into Anderson localization [99] and many-body localization [100]. Beyond these structural aspects, SREs also exhibit a fruitful interplay with non-stabilizerness and out-of-time-order correlators (OTOCs) [101, 102]. Higher-order extensions reveal additional links between OTOCs, nonstabilizerness, quantum chaos [101], and state certification [81], further underlining the versatility of SREs as a lens on quantum dynamics.

### 3 Probability densities of measures of non-stabilizerness

Due to normalization and invariance under phase change, the set of pure states on  $\mathcal{H}$  can be identified with  $\mathbb{C}P^{d-1}$ , the complex projective space of dimension  $d-1$  [82]. On this manifold, of real dimension  $2d-2$ , there is a unique, unitarily invariant measure  $d\psi$  [103, 104]. This measure is induced by the Haar measure  $dU$  on the corresponding unitary group  $U(d)$  when applied to a fiducial state  $|\psi_0\rangle \in \mathcal{H}$ , i.e.

$$\int_{\mathbb{C}P^{d-1}} d\psi f(|\psi\rangle) = \int_{U(d)} dU f(U|\psi_0\rangle), \quad (5)$$

for any integrable function  $f$ . A function from the set of pure states to  $\mathbb{R}$  becomes a real random variable when  $\mathbb{C}P^{d-1}$  is equipped with this uniform measure. Expectation values of  $f$  are computed with Eq. (5) via  $\mathbb{E}_\psi[f(|\psi\rangle)] = \mathbb{E}_U[f(U|\psi_0\rangle)] = \int dU f(U|\psi_0\rangle)$  [105–108]. In this work, we are interested in the probability density function (PDF) of the SRE when  $|\psi\rangle$  is distributed uniformly over the set of pure states, in the same spirit of entanglement [109]. In particular we will concentrate on the single qubit case, whence  $d=2$ , although we will make some comments for larger  $d$ . Since  $M_\alpha$  is a simple function of  $\Xi_\alpha$ , the PDF of  $M_\alpha$  can be obtained from that of  $\Xi_\alpha$  with a change of variable. Specifically,

$$P_{M_\alpha}(m) = |1 - \alpha| e^{(1-\alpha)m} P_{\Xi_\alpha}(e^{(1-\alpha)m}). \quad (6)$$

Hence, we are led to compute  $P_{\Xi_\alpha}(\xi)$  which can be formally written as

$$P_{\Xi_\alpha}(\xi) := \mathbb{E}_\psi[\delta(\Xi_\alpha(|\psi\rangle) - \xi)] = \int_{\mathbb{C}P^{d-1}} d\psi \delta(\Xi_\alpha(|\psi\rangle) - \xi). \quad (7)$$

In the following sections we are going to derive some of its features as well as exact results.

### 4 Van Hove singularities for general $\alpha$

From here on we focus on the single qubit case. A single qubit pure state can be written as

$$|\psi\rangle = \frac{\mathbb{1} + \mathbf{n} \cdot \boldsymbol{\sigma}}{2}, \quad (8)$$

where  $\mathbf{n} = (n_1, n_2, n_3)$  belongs to the Bloch's sphere as defined by the  $\ell^2$ -norm, i.e.  $\|\mathbf{n}\|_2 = 1$ , while  $\boldsymbol{\sigma} = (X, Y, Z)$  is a vector of Pauli matrices. The stabilizer purities in Eq. (3) become

$$\Xi_\alpha(|\psi\rangle) = \frac{1}{2} \sum_{P \in \mathbb{P}_1} |\langle \psi | P | \psi \rangle|^{2\alpha} = \frac{1 + \|\mathbf{n}\|_{2\alpha}^{2\alpha}}{2} \quad (9)$$

$$=: \frac{1 + N_\alpha}{2} \in \left[ \frac{1 + 3^{1-\alpha}}{2}, 1 \right], \quad (10)$$

<sup>1</sup> Stabilizer purities satisfy  $\Xi_{2\alpha}^{\frac{\alpha}{\alpha-1}} \leq \Xi_{2(\alpha+1)} \leq \Xi_{2\alpha}$ , see also [86].

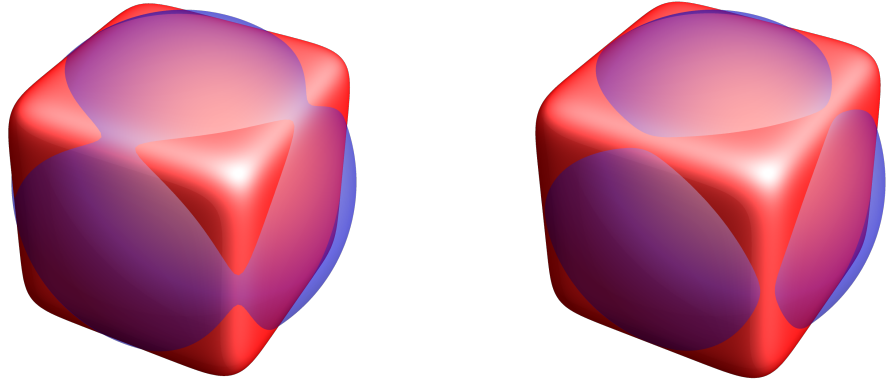


Figure 2: Intersection between  $\ell^{2\alpha}$  and  $\ell^2$ spheres, here for  $\alpha = 4$ . Left panel  $n = 0.12 < n_c$ , right panel  $n = 0.13 > n_c$ .

where we defined  $N_\alpha = \|\mathbf{n}\|_{2\alpha}^{2\alpha} = \sum_{j=1}^3 |n_j|^{2\alpha}$ . The maximum value of  $N_\alpha$  is one, attained when  $\mathbf{n}$  is  $\pm$  one of the three normalized coordinate vectors  $\hat{\mathbf{x}}, \hat{\mathbf{y}}, \hat{\mathbf{z}}$ , while the minimum of  $N_\alpha$  takes place when  $|n_1| = |n_2| = |n_3| = 1/\sqrt{3}$  for which  $N_\alpha = 3^{1-\alpha}$ . This explains the bound in Eq. (10). We focus our analysis on the quantity  $N_\alpha = \|\mathbf{n}\|_{2\alpha}^{2\alpha}$  and then turn back to the study of Eqns. (2-3) through a change of variable, i.e., via

$$P_{\Xi_\alpha}(\xi) = 2P_{N_\alpha}(2\xi - 1), \quad P_{M_\alpha}(m) = 2(\alpha - 1)e^{(1-\alpha)m}P_{N_\alpha}(2e^{(1-\alpha)m} - 1). \quad (11)$$

We use spherical coordinates to enforce the constraint  $\|\mathbf{n}\|_2 = 1$ , hence, using the coarea formula, the PDF of  $N_\alpha(\vartheta, \phi) = |\sin(\vartheta)|^{2\alpha} (|\cos(\phi)|^{2\alpha} + |\sin(\phi)|^{2\alpha}) + |\cos(\vartheta)|^{2\alpha}$  can be written as

$$\begin{aligned} P_{N_\alpha}(n) &= \int_0^{2\pi} \int_0^\pi \frac{\sin \vartheta d\vartheta d\phi}{4\pi} \delta(N_\alpha(\vartheta, \phi) - n) \\ &= \int_{N_\alpha^{-1}(n)} \frac{d\sigma_\lambda}{4\pi} \frac{1}{\|\nabla N_\alpha(\vartheta(\lambda), \phi(\lambda))\|_2}, \end{aligned} \quad (12)$$

with  $d\sigma_\lambda = \sqrt{\left(\frac{d\vartheta}{d\lambda}\right)^2 + \sin^2 \vartheta \left(\frac{d\phi}{d\lambda}\right)^2} d\lambda$  the induced surface measure on the level set, a one-dimensional set in this case.

At this point we would like to remark that Eq. (12) for  $P_{N_\alpha}(n)$  is exactly the density of states (DOS) of a system with energy dispersion given by  $N_\alpha(\vartheta, \phi)$ , for which the coordinates  $\boldsymbol{\vartheta} := (\vartheta, \phi)$  play the role of momenta and whose first Brillouin zone is the sphere. From this observation, we can already draw some conclusions from the vast existing literature regarding the behavior of the density of states in solids. Eq. (12) suggests that one may have divergencies of the DOS, called Van Hove singularities, at locations where the gradient  $\nabla N_\alpha$  is zero (the dispersion is flat). Such critical points correspond to local maxima or minima of  $N_\alpha$  or saddle points. Generally, in two dimensions, as is the dimension of the sphere, locations of maxima or minima of the dispersions do not give rise to a divergent DOS, but rather simply step-wise singularities corresponding to the behavior at the edge. Instead saddle points give rise to logarithmic singularities in the DOS [110]. In the following we will carefully prove that these predictions are indeed correct.

The integration region in Eq. (12) is the intersection between the  $\ell^{2\alpha}$  sphere of radius  $n^{1/2\alpha}$ , i.e.  $|n_1|^{2\alpha} + |n_2|^{2\alpha} + |n_3|^{2\alpha} = n$ , and the  $\ell^2$  sphere of radius one, i.e.  $n_1^2 + n_2^2 + n_3^2 = 1$ . Since  $\alpha > 1$  the  $\ell^{2\alpha}$  sphere resembles a cube with rounded edges, see Figure 2. When  $n$  is close to one, the intersection gives rise to eight closed loops at the vertices of this rounded cube. Instead, when  $n$  is close to the lower bound  $3^{1-\alpha}$ , the intersection gives rise to closed loops around the faces of the smoothed cube so that in this case there are six closed loops, see Figure 3. As  $n$  varies smoothly from the lower bound to the upper bound, there must be a critical value  $n_c$  where the six loops and the eight loops coexist. It is natural to suppose that for this value of  $n$ , the gradient of  $N_\alpha$  vanishes at some point. Notice that *critical points* of the function  $N_\alpha = \|\mathbf{n}\|_{2\alpha}^{2\alpha}$

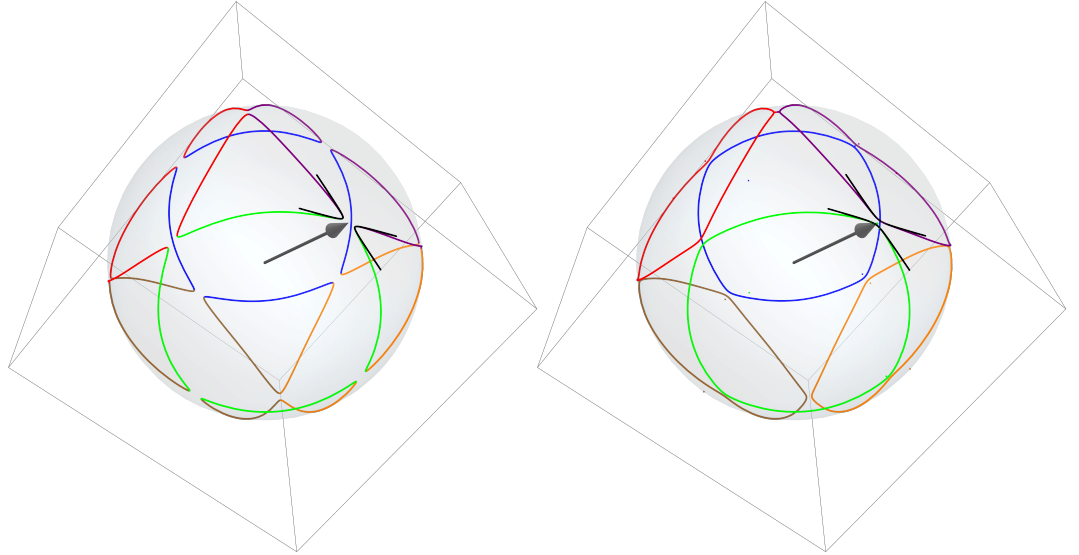


Figure 3: Integration regions to compute the stabilizer purity PDF for  $\alpha = 4$ . The grey arrow is the critical point  $\mathbf{n}_c = (1/\sqrt{2}, 1/\sqrt{2}, 0)$  and the black curves are the hyperbolae where integration takes place for  $n$  close to  $n_c = 1/8$ . Left panel  $n = 0.124 < n_c$ , right panel  $n = 0.126 > n_c$ .

under the constraint  $\|\mathbf{n}\|_2^2 = 1$ , that is, points where the gradient is zero, correspond to *isolated points* on the intersection of the unit sphere and the  $\ell_{2\alpha}$ -sphere defined by  $N_\alpha = n$ . The full set of solutions of the system

$$\|\mathbf{n}\|_2^2 = 1, \quad \text{and} \quad \|\mathbf{n}\|_{2\alpha}^{2\alpha} = n, \quad (13)$$

is generally a *1-dimensional manifold* (a curve) embedded in the sphere, as it represents the intersection of two smooth surfaces in  $\mathbb{R}^3$ . Therefore, the solutions form continuous, smooth curves, except at critical points where these curves can change topology or number of connected components, as shown in Fig. 3. In spherical coordinates, using the substitution  $s = \sin(\vartheta)^2$ , the equation  $N_\alpha(\vartheta, \phi) = n$  reduces to a polynomial of degree  $\alpha$  in  $s$ . Therefore, in principle, solutions are available in terms of radicals (after a careful examination of various positivity conditions) for  $\alpha = 2, 3, 4$ , but the resulting expressions for the integral in Eq. (12) are kilometric and unpractical for  $\alpha > 2$ . We will give an explicit integral representation for  $P_{N_\alpha}(n)$  for  $\alpha = 2$  in Section 5 using a different method.

We first find the critical points of the function  $N_\alpha(\mathbf{n})$  where  $\mathbf{n} \in \mathbb{S}^2 = \{\mathbf{n} | \|\mathbf{n}\|_2 = 1\}$ , i.e. points on the sphere where  $\nabla N_\alpha = 0$ . In order to do so, we enforce the constraint via Lagrange multipliers and define the following Lagrangian:

$$\mathcal{L}(n_1, n_2, n_3, \lambda) = \sum_{i=1}^3 |n_i|^{2\alpha} - \lambda \left( \sum_{i=1}^3 n_i^2 - 1 \right). \quad (14)$$

Setting the partial derivatives to zero we get

$$\frac{\partial \mathcal{L}}{\partial n_i} = 2\alpha \text{sign}(n_i) |n_i|^{2\alpha-1} - 2\lambda n_i = 0. \quad (15)$$

The solution of the above equation is either  $n_i = 0$ , or, assuming  $n_i \neq 0$ ,

$$\alpha |n_i|^{2\alpha-2} = \lambda, \quad (16)$$

which implies that all nonzero components of  $\mathbf{n}$  have the same absolute value. The function  $N_\alpha : \mathbb{S}^2 \rightarrow \mathbb{R}$  is invariant under the action of the *hyperoctahedral group*  $G = S_3 \times \mathbb{Z}_2^3$  [111], which consists of all permutations and sign changes of the components of  $\mathbf{n}$ . By Palais principle [112], critical points of  $N_\alpha$  must occur in  $G$ -symmetric configurations, i.e., vectors that are invariant under some subgroup of  $G$ . Up to symmetry, the critical points of  $N_\alpha$  on  $\mathbb{S}^2$  fall into three classes:

$$\begin{aligned} C_1 &= \{(\pm 1, 0, 0), (0, \pm 1, 0), (0, 0, \pm 1)\}, \quad N_\alpha = 1 \\ C_2 &= \left\{ \left( \pm \frac{1}{\sqrt{2}}, \pm \frac{1}{\sqrt{2}}, 0 \right), \left( \pm \frac{1}{\sqrt{2}}, 0, \pm \frac{1}{\sqrt{2}} \right), \left( 0, \pm \frac{1}{\sqrt{2}}, \pm \frac{1}{\sqrt{2}} \right) \right\}, \quad N_\alpha = 2^{1-\alpha} \\ C_3 &= \left\{ \left( \pm \frac{1}{\sqrt{3}}, \pm \frac{1}{\sqrt{3}}, \pm \frac{1}{\sqrt{3}} \right) \right\}, \quad N_\alpha = 3^{1-\alpha} \end{aligned} \quad (17)$$

There are respectively 6, 12 and 8 points in each class. The first, respectively third, class correspond to absolute maximum, respectively minimum, of  $N_\alpha$ , namely stabilizer states and maximal magic states ( $|T\rangle$ -type states in [6]). The corresponding values of  $N_\alpha$ ,  $1$ ,  $3^{1-\alpha}$ , are the edge of the support of  $P_{N_\alpha}(n)$ ,  $[3^{1-\alpha}, 1]$ , and for what we have said previously  $P_{N_\alpha}(n)$  has a simple stepwise singularity around these points where it raises from zero to a finite value at the lower edge or goes to zero from a finite value at the upper edge. The 12 points in the second class, taking place at  $n = n_c := 2^{1-\alpha}$ , are precisely the locations where the 8 loops for  $n < n_c$  touch the six loops for  $n > n_c$ . The corresponding states are precisely the so called  $|H\rangle$ -states defined first in [6], given by the Clifford orbit of  $|H\rangle \langle H| = \frac{1}{2} \left( \mathbb{1} + \frac{X+Z}{\sqrt{2}} \right)$ . As we will show below, these are saddle points of  $N_\alpha$  and give rise to logarithmic, Van Hove singularities in  $P_{N_\alpha}(n)$ . Notice that the position of the singularity is given by

$$\Xi_\alpha|_c = \frac{1 + 2^{1-\alpha}}{2}, \quad M_\alpha|_c = \frac{1}{1-\alpha} \ln \left( \frac{1 + 2^{1-\alpha}}{2} \right). \quad (18)$$

In order to prove this claim we need to find, to leading order, the curves resulting from the intersection of  $N_\alpha = n$  and  $\|\mathbf{n}\|_2^2 = 1$  when  $n$  is close to  $n_c$ , for generic  $\alpha \geq 2$ . We fix  $\mathbf{n}_c = (1/\sqrt{2}, 1/\sqrt{2}, 0)$ , so in spherical coordinate we set  $\vartheta = \pi/2 + \vartheta'$  and  $\phi = \pi/4 + \phi'$ , where  $\vartheta' = \phi' = 0$  corresponds to  $\mathbf{n}_c$ . Since  $\alpha > 1$  we obtain, up to leading order

$$\begin{aligned} \|\mathbf{n}\|_{2\alpha}^{2\alpha} &\simeq 2^{1-\alpha} + 2^{2-\alpha} \alpha(\alpha-1) \phi'^2 - 2^{1-\alpha} \alpha \vartheta'^2 \\ &= n_c + 2^{2-\alpha} \alpha(\alpha-1) \phi'^2 - 2^{1-\alpha} \alpha \vartheta'^2, \end{aligned} \quad (19)$$

explicitly showing that  $\mathbf{n}_c$  is a saddle point (the linear terms are zero and the Hessian has a positive and a negative eigenvalue). Equating the above to  $n$  we see that the constraint becomes the equation of an hyperbola in the variables  $\phi', \vartheta'$ :

$$2^{2-\alpha} \alpha(\alpha-1) \phi'^2 - 2^{1-\alpha} \alpha \vartheta'^2 = n - n_c. \quad (20)$$

For  $n > n_c$  we can write

$$\phi' = \pm \sqrt{\frac{n - n_c}{2^{2-\alpha} \alpha(\alpha-1)} + \frac{1}{2(\alpha-1)}} \vartheta'. \quad (21)$$

Exactly at  $n = n_c$  the hyperbolae degenerate into two straight lines (the asymptotes for  $n \neq n_c$ )

$$\phi' = \pm \sqrt{\frac{1}{2(\alpha-1)}} \vartheta', \quad (22)$$

however on these lines the integrand is infinite so we need to keep  $n \neq n_c$ . We now expand the gradient around the same point and get

$$\|\nabla N_\alpha\|_2^2 \simeq 4^{3-\alpha} (\alpha-1)^2 \alpha^2 \phi'^2 + 4^{2-\alpha} \alpha^2 \vartheta'^2, \quad (23)$$

which, after imposing the constraint Eq. (21), becomes

$$\|\nabla N_\alpha\|_2^2 \simeq 2^\alpha 4^{2-\alpha} \alpha(\alpha-1)(n - n_c) + 4^{2-\alpha} \alpha^2 (2\alpha-1) \vartheta'^2. \quad (24)$$

Plugging in the line element and expanding to leading order, we obtain the most diverging contribution to the integral Eq. (12) for  $n \rightarrow n_c$

$$\int_{-\delta}^{\delta} d\vartheta' \frac{1}{\sqrt{2^\alpha 4^{2-\alpha} \alpha(\alpha-1)(n - n_c) + 4^{2-\alpha} \alpha^2 (2\alpha-1) \vartheta'^2}} = -\frac{\ln(n - n_c)}{2^{2-\alpha} \alpha \sqrt{2\alpha-1}} + O(1), \quad (25)$$

where  $\delta$  is any small positive constant and we used the following identity valid for  $\epsilon \rightarrow 0$  (and  $a, b > 0$ ), [113]

$$\int_{-\delta}^{\delta} \frac{dy}{\sqrt{a\epsilon + by^2}} = -\frac{\ln(\epsilon)}{\sqrt{b}} + O(1). \quad (26)$$

Overall we obtain, for  $n \rightarrow n_c^+$

$$P_{N_\alpha}(n) \propto -\ln(n - n_c). \quad (27)$$

For  $n < n_c$  the roles of  $\phi'$  and  $\vartheta'$  are reversed. Proceeding analogously we obtain, for  $n \rightarrow n_c$ ,

$$P_{N_\alpha}(n) \propto -\ln|n - n_c|. \quad (28)$$

That is, the anticipated logarithmic divergence of the PDF when  $n \rightarrow n_c$ . Similar expansions show that, close to the minima or maxima of  $N_\alpha$ , the integrand in Eq. (12) has only square root singularities, which are integrable and give rise to a finite  $P_{N_\alpha}(n)$ .

The same logarithmic divergence can be observed for the SRE Eq. (2), and the SP Eq. (3), using Eq. (11) (see Appendix B)

$$P_{\Xi_\alpha}(\xi) \propto -\ln \left| \xi - \frac{1+n_c}{2} \right| \quad P_{M_\alpha}(m) \propto -\ln \left| m - \frac{1}{1-\alpha} \ln \left( \frac{1+n_c}{2} \right) \right|. \quad (29)$$

## 5 Case $\alpha = 2$

The case  $\alpha = 2$  can be carried out in greater detail, and it is also the most important as it corresponds to the simplest non-stabilizer monotone. We obtain the PDF of  $N_2 = \|\mathbf{n}\|_4^4$  by first computing its characteristic function and then Fourier transforming. First, going to spherical coordinates, we write

$$\|\mathbf{n}\|_4^4 = \sin(\vartheta)^4 + \cos(\vartheta)^4 - \frac{\sin(2\phi)^2}{2} \sin(\vartheta)^4, \quad (30)$$

so that the characteristic function of  $N_2$  reads

$$\chi_{N_2}(k) = \mathbb{E} \left[ e^{ikN_2} \right] \quad (31)$$

$$= \int_0^{2\pi} \int_0^\pi \frac{d\phi d\vartheta \sin(\vartheta)}{4\pi} \exp \left[ -ik \left( \sin(2\phi)^2 / 2 \right) \sin(\vartheta)^4 + ik \cos(\vartheta)^4 + ik \sin(\vartheta)^4 \right]. \quad (32)$$

Now we use

$$\int_0^{2\pi} \frac{d\phi}{2\pi} e^{-iy \sin(2\phi)^2} = e^{-iy/2} J_0(y/2), \quad (33)$$

where  $J_0$  is the Bessel function of the first kind and  $y = k \sin(\vartheta)^4 / 2$ , whence we obtain

$$\chi_{N_2}(k) = \frac{1}{2} \int_0^\pi d\vartheta \sin(\vartheta) \exp \left[ ik \cos(\vartheta)^4 + ik \frac{3}{4} \sin(\vartheta)^4 \right] J_0 \left( \frac{k \sin(\vartheta)^4}{4} \right). \quad (34)$$

We now perform a Fourier transform to obtain the PDF. We use the following identity, with  $\theta$  the Heaviside function [113]

$$\int_{\mathbb{R}} e^{ikx} J_0(ax) dx = 2 \frac{\theta(1-|k/a|)}{\sqrt{a^2-k^2}} = 2 \frac{\theta(a-|k|)}{\sqrt{a^2-k^2}}, \quad \text{for } a > 0, \quad (35)$$

with  $x = \cos(\vartheta)$  and

$$a(x) = (1-x^2)^2 \quad (36)$$

$$k(x) = 3(1-x^2)^2 + 4x^4 - 4n. \quad (37)$$

Hence, we obtain the final form of the PDF using the parity of the integrand

$$P_{N_2}(n) = \frac{4}{\pi} \int_0^1 dx \frac{\theta \left( (1-x^2)^2 - \left| 3(1-x^2)^2 + 4x^4 - 4n \right| \right)}{\sqrt{(1-x^2)^4 - \left( 3(1-x^2)^2 + 4x^4 - 4n \right)^2}}. \quad (38)$$

For  $n \in [1/3, 1/2)$  the  $\theta$  constraints the integration in  $x \in [x_-, x_+]$ , where  $x_\pm$  are the roots in  $[0, 1]$  of  $a(x) = k(x)$  which are

$$x_\pm = \left( \frac{1 \pm \sqrt{6n-2}}{3} \right)^{1/2}. \quad (39)$$

For  $n \in (1/2, 1]$  the integration region  $|k(x)| < a(x)$  becomes  $x \in [0, y_-)$  and  $x \in (y_+, 1]$ . Where  $y_\pm$  are the roots of  $a(x) = -k(x)$  in  $[0, 1]$ . These are

$$y_\pm = \left( \frac{1 \pm \sqrt{2n-1}}{2} \right)^{1/2}. \quad (40)$$

All in all we obtain (see figure 4)

$$P_{N_2}(n) = \begin{cases} \frac{4}{\pi} \int_{x_-}^{x_+} dx \frac{1}{\sqrt{(1-x^2)^4 - (3(1-x^2)^2 + 4x^4 - 4n)^2}} & \text{for } n \in [1/3, 1/2) \\ \frac{4}{\pi} \left( \int_0^{y_-} dx + \int_{y_+}^1 dx \right) \frac{1}{\sqrt{(1-x^2)^4 - (3(1-x^2)^2 + 4x^4 - 4n)^2}} & \text{for } n \in (1/2, 1] \end{cases}. \quad (41)$$

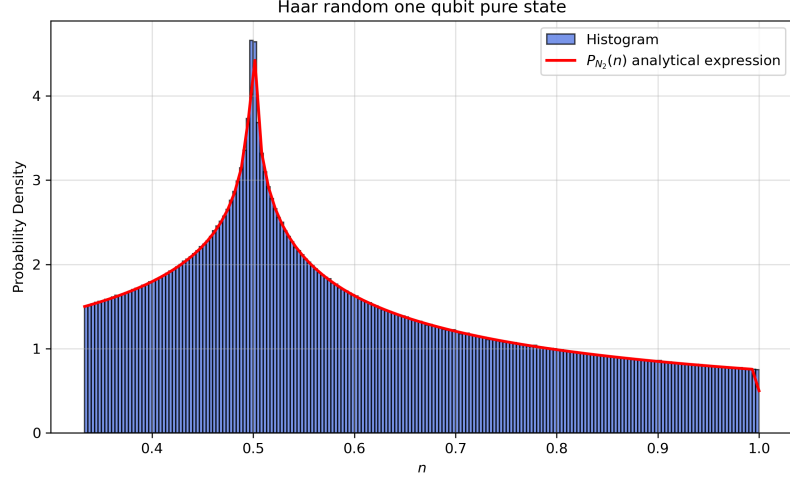


Figure 4: In blue the numerical probability density function of  $P_{N_2}(n)$  using  $N_{sample} = 10^7$  one-qubit random pure states extracted according to the Haar measure. In red the theoretical analytical distribution Eq. (41).

Moreover  $P_{N_2}(n) = 0$  for  $n < 1/3$  and  $n > 1$  and is infinite for  $n = 1/2$ . The PDF of the two-SRE (and of the two-stabilizer purity) can be obtained via Eq. (11) and the result is shown in Fig. 1.

In particular, using Eq. (41), we obtain the exact mean value of the SRE for one qubit:

$$\mathbb{E}_\psi[M_2(\psi)] = \int_0^1 dx \ln \left( \frac{16}{7x^4 - 6x^2 + 4\sqrt{3}x^8 - 5x^6 + 8x^4 - 5x^2 + 3 + 7} \right) \simeq 0.228921, \quad (42)$$

see Appendix A for more details.

In the remainder of this chapter we explicitly check the form of the divergence of  $P_{N_2}(n)$  for  $n \rightarrow n_c$  using the explicit expression (41). Note that the argument of the square root can be written as

$$-48(x^2 - x_-^2)(x^2 - x_+^2)(x^2 - y_-^2)(x^2 - y_+^2), \quad (43)$$

hence when  $x$  is close to the border of integration,  $x_\pm$  the integrand behaves as

$$\frac{1}{\sqrt{|x - x_\pm|}}, \quad (44)$$

which is integrable and leads to a bounded  $P_{N_2}(n)$ . However, when  $n \rightarrow 1/2^-$  the integrand develops another singularity. In this case  $y_\pm^2 \rightarrow 1/2$ , and around  $x = y_-|_{n=1/2} = 1/\sqrt{2}$ , the integrand behaves as

$$\frac{1}{\left| x - \frac{1}{\sqrt{2}} \right|}, \quad (45)$$

which is not integrable and leads to a divergence of  $P_{N_2}(n)$ . The same happens for  $n \rightarrow 1/2^+$ . We can guess that the divergence will be of logarithmic type, however let us proceed with order. When  $y_\pm^2 \rightarrow 1/2$  and  $x$  is close to  $1/\sqrt{2}$ , the integrand (a part from a factor  $4/\pi$ ) behaves as (expanding the argument of the square root up to second order around  $x = 1/\sqrt{2}$ ),

$$\frac{1}{2\sqrt{(x^2 - y_-^2)(x^2 - y_+^2)}} \simeq \frac{1}{2\sqrt{\frac{(1-2n)}{4} + 2\left(x - \frac{1}{\sqrt{2}}\right)^2}}. \quad (46)$$

This function can be integrated in any interval containing  $x = 1/\sqrt{2}$  leading to a logarithmic divergence. Specifically, using Eq. (26), we obtain (without the factor  $4/\pi$ )

$$-\frac{1}{2\sqrt{2}} \ln \left( \frac{1}{2} - n \right). \quad (47)$$

Summing up both divergencies and multiplying by  $4/\pi$  we obtain the overall behavior for  $n \rightarrow 1/2^-$

$$P_{N_2}(n) = -\frac{3}{\sqrt{2}\pi} \ln \left( \frac{1}{2} - n \right) + O(1). \quad (48)$$

The behavior for  $n \rightarrow 1/2^+$  can be obtained in a similar way. Exactly at  $n = 1/2$ , there are non-integrable singularities at  $x = 0$ ,  $x = y_-$  and  $x = y_+$ . For the singularity around zero we can approximate the integrand as

$$\frac{1}{\sqrt{8}\sqrt{x^2 + (n - \frac{1}{2})}}. \quad (49)$$

From this we obtain, for  $n \rightarrow 1/2^+$ , integrating on any interval  $[0, \delta]$ , with  $\delta > 0$ ,

$$\int_0^\delta \frac{dx}{\sqrt{8}\sqrt{x^2 + (n - \frac{1}{2})}} = -\frac{1}{4\sqrt{2}} \ln\left(n - \frac{1}{2}\right) + O(1). \quad (50)$$

For the singularities at  $x = y_\pm$  we can approximate the integrand (setting  $y_\pm^2 = 1/2$  and  $x$  close to  $1/\sqrt{2}$ ) as

$$\frac{1}{2\sqrt{2}\left|x - \frac{1}{\sqrt{2}}\right|}. \quad (51)$$

Integrated around  $y_-$  gives (for any  $\delta < y_-$ )

$$\int_\delta^{y_-} \frac{dx}{2\sqrt{2}\left|x - \frac{1}{\sqrt{2}}\right|} = -\frac{1}{4\sqrt{2}} \ln\left(n - \frac{1}{2}\right) + O(1). \quad (52)$$

The integral around  $y_+$  gives the same result (for any  $\delta > y_+$ ):

$$\int_{y_+}^\delta \frac{dx}{2\sqrt{2}\left|x - \frac{1}{\sqrt{2}}\right|} = -\frac{1}{4\sqrt{2}} \ln\left(n - \frac{1}{2}\right) + O(1). \quad (53)$$

Summing up all three contributions and multiplying by  $4/\pi$  we obtain the same divergence as for  $n \rightarrow 1/2^-$ . So, all in all we obtain, for  $n \rightarrow 1/2$

$$P_{N_2}(n) = -\frac{3}{\sqrt{2}\pi} \ln\left|n - \frac{1}{2}\right| + O(1). \quad (54)$$

## 6 Absence of Van Hove singularities for larger Hilbert spaces

One can ask what happens in the case of larger Hilbert spaces such as for qudit or multi-qubit systems. The construction of Eq. (10) can be generalized to any Hilbert space of dimension  $d$ . First, one writes the general pure state in  $\mathbb{C}P^{d-1}$  in terms of the Hurwitz parametrization [103], via  $2d - 2$  real angles  $\vartheta, \phi$ . If the system is a multi-qubit system, e.g.  $d = 2^L$ , one defines the vector  $\mathbf{n} = (n_1, \dots, n_{d^2-1})$  via

$$n_j(\vartheta, \phi) = \text{Tr}(P_j \psi), \quad j = 1, \dots, d^2 - 1, \quad (55)$$

for any Pauli string  $P_j$  except the identity, that is  $P_j \in \mathbb{P}_L \setminus \{\mathbb{1}\}$ . Then, for  $\alpha \geq 2$ , one defines

$$\Xi_\alpha(\vartheta, \phi) = \frac{1}{d} (1 + \|\mathbf{n}(\vartheta, \phi)\|_{2\alpha}^{2\alpha}) =: \frac{1}{d} (1 + N_\alpha(\vartheta, \phi)), \quad (56)$$

and we are led to study  $P_{N_\alpha}(n)$  the Haar-induced probability density of  $N_\alpha$ . The problem becomes that of estimating the DOS of a system with dispersion  $N_\alpha(\vartheta, \phi)$  where the "Brillouin zone", here  $\mathbb{C}P^{d-1}$ , has dimension  $D = 2d - 2$ . Now we borrow the result that, if the Hessian of  $N_\alpha$  is never identically vanishing (in other words, the critical points of  $N_\alpha$  are *ordinary*), one does not have a Van Hove singularity of the DOS for  $D \geq 3$  [110], meaning  $d \geq 2.5$ . Therefore, modulo unlikely accidental cancelation of the Hessian,  $d = 2$  is the only dimension for which van Hove singularities should be observed. Indeed, the absence of divergencies for  $n > 1$  is verified by our numerical simulations, see Fig. 5.

In case the system consists of one qudit of dimension  $q$ , one can extend the notion of the Pauli group to that of the Weyl-Heisenberg group, namely the set of displacement operators and integer powers of the phase factor  $\omega$ :

$$\mathcal{W}(q) = \{\omega^s D_{\mathbf{a}} : s \in \mathbb{Z}_q, \mathbf{a} \in \mathbb{Z}_q^2\}. \quad (57)$$

Thus, in analogy to the qubits case, the stabilizer purities in the case of qudit is defined as [114]

$$\Xi_\alpha(|\psi\rangle) = \frac{1}{q} \sum_{D_{\mathbf{a}} \in \mathcal{W}(d)} |\text{Tr}(D_{\mathbf{a}} \psi)|^{2\alpha}, \quad (58)$$

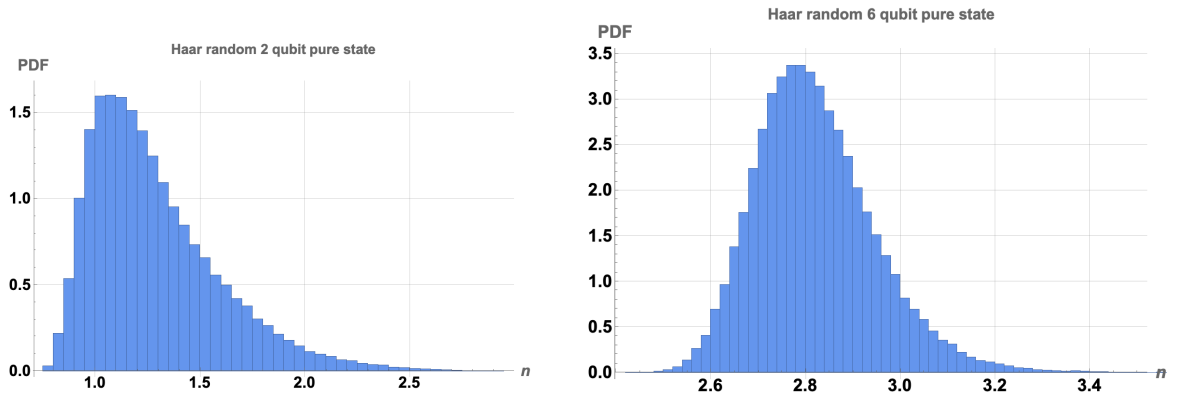


Figure 5: Probability density function of  $P_{N_2}(n)$  for 2 and 6 qubits extracted numerically for  $N_{sample} = 2 \times 10^5$  pure Haar random states.

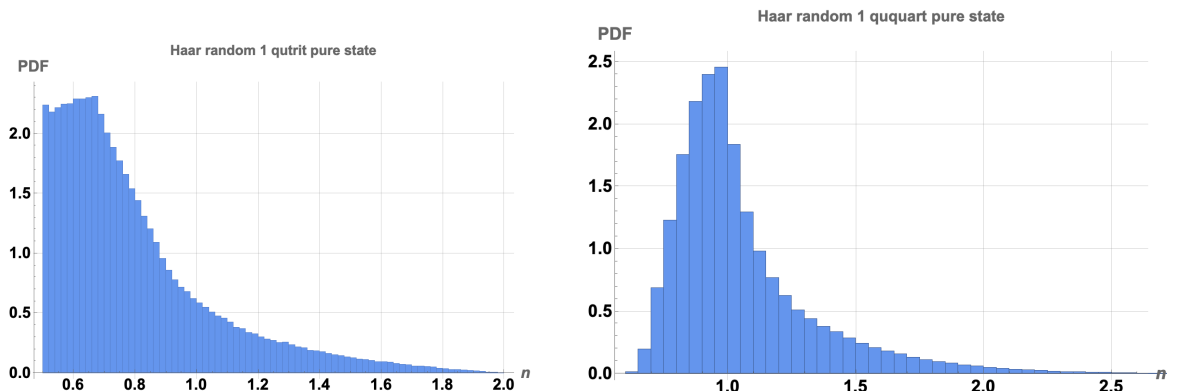


Figure 6: Probability density function of  $P_{N_2}(n)$  for one qutrit and ququart extracted numerically for  $N_{sample} = 4 \times 10^5$  pure Haar random states, where we used the generalization of SREs for the qudit case [114].

and the SREs

$$M_\alpha(|\psi\rangle) = \frac{1}{1-\alpha} \ln \Xi_\alpha(|\psi\rangle). \quad (59)$$

Finally, in this context  $N_\alpha(|\psi\rangle) = q \Xi_\alpha(|\psi\rangle) - 1$  (see Appendix C for details), and after Hurwitz parametrization we are led formally to a similar problem as before. For what we have said, we do not expect divergencies in the PDF of  $N_\alpha$  for  $q \geq 2.5$ , and at the same time we expect a less smooth behaviour of the PDF the smaller the dimension. These features can be appreciated in our numerical simulations shown in Fig. 6.

## 7 General considerations on single qubit PDF's

For what we have said previously, borrowing results for the density of states in solids, one may be led to conclude that van Hove singularities in  $d = 2$  are present in the PDF,  $P_X(x)$ , of any quantity  $X$  defined on the Bloch sphere, or, in other words, that in  $d = 2$ , divergencies are the norm rather than the exception. However, we should remember that the condition for logarithmic divergence in  $d = 2$ , is that the function  $X(\vartheta, \phi)$  has a saddle point on the sphere. Moreover, one should be careful that the PDF's that we are considering here are defined on a curved base manifold, the (Bloch) sphere, as opposed to a flat manifold as is the standard case for the density of states in solids. In practice, one has to take into account the effect of the term  $\sin(\vartheta)$  in the measure in Eq. (12). See [115] for some concrete examples in the case of different measures of entanglement.

To illustrate these subtleties, we consider then two other important quantities that can be defined on the single-qubit space. The first one is the expectation value  $A = \langle \psi | \mathcal{A} | \psi \rangle$  of an observable  $\mathcal{A}$ . The PDF,  $P_A(a)$ , of an observable  $\mathcal{A}$ , when  $|\psi\rangle$  is uniformly distributed in  $\mathbb{C}P^{d-1}$ , has been computed in [116]. For  $d = 2$  the

PDF has the following expression:

$$P_A(a) = \frac{1}{a_2 - a_1} \mathbb{1}_{[a_1, a_2]}(a), \quad (60)$$

where  $a_1 < a_2$  are the eigenvalues of  $\mathcal{A}$ , and  $\mathbb{1}_{[a_1, a_2]}(a)$  is the characteristic function of the interval  $[a_1, a_2]$ . In other words,  $P_A(a)$  is the uniform distribution supported in  $[a_1, a_2]$ . The explicit form of  $A(\vartheta, \phi)$  depends on the observable. However, upon diagonalization, it can always be cast in the form

$$U^\dagger \mathcal{A} U = \text{diag}(\mathcal{A}) = \frac{a_1 + a_2}{2} \mathbb{1} + \frac{a_1 - a_2}{2} Z, \quad (61)$$

so that after a rotation, a shift, and a scale transformation, one is led to consider  $Z(\vartheta, \phi) = \cos(\vartheta)$  (or any other Pauli matrix for that matter). The problem becomes one-dimensional, and according to the standard classification one would expect square root singularities at the extrema of  $\cos(\vartheta)$ . However, the measure is not  $d\vartheta$  but rather  $(1/2) \sin(\vartheta) d\vartheta$  and a single change of variable,  $x = \cos(\vartheta)$ , leads to the result (60).

We now consider another quantity that can be defined on the Bloch sphere. Namely the *coherence* of the state  $|\psi\rangle$  measured using the computational basis as reference basis. Using the  $\ell^1$  norm, a measure of coherence in the basis  $\{|i\rangle\}$  of the mixed state  $\rho$ , is given by [117]

$$C(\rho) = \sum_{i \neq j} |\langle i | \rho | j \rangle|, \quad (62)$$

which, for a single qubit, reduces to  $C = 2|\rho_{0,1}|$ . Using the standard parameterization of the sphere one obtains  $C(\psi) = |\sin \vartheta|$ , which does not depend on  $\phi$ . Again, the problem is reduced to computing a one dimensional DOS and one can expect a square root singularity at the location where  $C(\psi)$  is maximal or minimal. Indeed, in this case, the singularity is not absorbed by the measure, and an explicit calculation (see Appendix D) gives

$$P_C(c) = \frac{c}{\sqrt{1-c^2}} \mathbb{1}_{[0,1]}(c), \quad (63)$$

which has a square root singularity at  $c = 1$ , i.e. at the maximum of  $C$ .

This short discussion seems to indicate that, out of three physically interesting quantities that can be defined on a qubit, only the SRE shows a logarithmic singularity in its PDF. Moreover, the PDF of another measure of non-stabilizerness, the magic by trace distance, has been recently investigated numerically [80]. The results in [80] show a singularity also occurring at the  $|H\rangle$ -states [118] and are compatible with a logarithmic divergence at this critical value. This, if confirmed, indicates that the logarithmic divergence is a genuine feature of non-stabilizerness which does not depend on the particular monotone.

## 8 Incompatibility deficit

So far, we have studied for a single qubit the distribution of the stabilizer Rény entropy and traced it back to that of the stabilizer purity. The stabilizer purity has a clear information-theoretic [78] and operational [81] interpretation. Remarkably, in the case of one-qubit systems, it has also a very clear interpretation in terms of fundamental quantum mechanics concepts. As is well known, one of the defining features of quantum mechanics lies in the existence of non-compatible observables and bases. This is, for example, demonstrated in fundamental thought experiments such as the cascaded Stern-Gerlach experiments [119], where one shows that, for a two-level system, there are three maximally incompatible bases, typically referred to as the  $X, Y, Z$  bases, corresponding to measurements characterized by statistics that go beyond classical results. The fact that there are infinitely partially incompatible bases is usually overlooked as they show the same behavior, just in a lesser fashion. Now we argue that for one qubit, partial incompatibility is in fact directly related to non-stabilizerness. Since compatible quantities commute, we define the  $\alpha$ -incompatibility as

$$\Gamma_\alpha(\psi) := \sum_{j=1}^3 \|\psi, \sigma_j\|_{2\alpha}^{2\alpha} = \frac{1}{2^{2\alpha}} \sum_{j=1}^3 \|\mathbf{n} \cdot \boldsymbol{\sigma}, \sigma_j\|_{2\alpha}^{2\alpha}, \quad (64)$$

with  $\boldsymbol{\sigma} = \{X, Y, Z\}$  and  $\|\mathbf{n}\|_2 = 1$ , where we identify  $\psi = \frac{\mathbb{1} + \mathbf{n} \cdot \boldsymbol{\sigma}}{2}$ . This is (proportional to) the average non compatibility of the single qubit state with respect to the Pauli operators  $\sigma_j$  as measured by the  $2\alpha$ -norm of the commutator. In order to compute the generic explicit formula, let us start by noticing that

$$C_j := [\mathbf{n} \cdot \boldsymbol{\sigma}, \sigma_j] = \sum_{k=1}^3 n_k [\sigma_k, \sigma_j] = 2i \sum_{k=1}^3 n_k \varepsilon_{kjl} \sigma_l \equiv 2i(\mathbf{n} \times \mathbf{e}_j) \cdot \boldsymbol{\sigma}, \quad (65)$$

where  $e_j$  is the  $j$ -th standard basis vector and  $v_j := \mathbf{n} \times e_j$  is the vector whose components are  $(v_j)_l = n_k \varepsilon_{kjl}$ . Observe that  $\|v_j\|_2^2 = \|\mathbf{n} \times e_j\|_2^2 = \|\mathbf{n}\|_2^2 - n_j^2$ . Recall that the shatten norm is defined as  $\|A\|_{2\alpha}^{2\alpha} = \text{Tr}[(A^\dagger A)^\alpha]$ , hence

$$C_j^\dagger C_j = 4(v_j \cdot \boldsymbol{\sigma})^2 = 4\|v_j\|_2^2 \mathbb{1}, \quad (66)$$

which means

$$\sum_{j=1}^3 \text{Tr}[(C_j^\dagger C_j)^\alpha] = \sum_{j=1}^3 2^{2\alpha+1} \|v_j\|_2^{2\alpha} = \sum_{j=1}^3 2^{2\alpha+1} (\|\mathbf{n}\|_2^2 - n_j^2)^\alpha. \quad (67)$$

Finally, we have the following expression in terms of stabilizer purities for integer values of  $\alpha$

$$\Gamma_\alpha(\psi) = 2 \sum_{j=1}^3 (\|\mathbf{n}\|_2^2 - n_j^2)^\alpha = 2 \sum_{s=0}^{\alpha} \binom{\alpha}{s} (-1)^s \|\mathbf{n}\|_{2s}^{2s} = 2 \sum_{s=0}^{\alpha} \binom{\alpha}{s} (-1)^s (2\Xi_s(\psi) - 1). \quad (68)$$

In particular, for  $\alpha = 1, 2$ , one obtains

$$\Gamma_1(\psi) = 4\|\mathbf{n}\|_2^2 = 4, \quad \Gamma_2(\psi) = 4\Xi_2(\psi) = 4(1 - M_2^{\text{lin}}(\psi)). \quad (69)$$

This result shows that the incompatibility of order two  $i_s$  is proportional to the stabilizer purity and the linear stabilizer entropy is an incompatibility deficit. Hence, the PDF of the two-incompatibility is readily obtained from the PDF of two-stabilizer purity,  $\Xi_2$ . Moreover, Eq. (69) implies that stabilizer states host the maximum amount of incompatibility with respect the  $X, Y, Z$  directions while non-stabilizerness is a deficit of such incompatibility. Notice that the  $X, Y, Z$  are the same that define the notion of stabilizer states, that is, the Pauli algebra of one qubit.

A similar result can be obtained in the case of multiple-qubit systems, generalizing Eq. (64) to

$$\Gamma_\alpha(\psi) = \sum_{P \in \mathcal{P}_L} \|\llbracket \psi, P \rrbracket\|_{2\alpha}^{2\alpha}, \quad (70)$$

in which case one obtains (see Appendix E)

$$\Gamma_\alpha(\psi) = 2d \sum_{s=0}^{\alpha} \binom{\alpha}{s} (-1)^s \Xi_s(\psi), \quad \Gamma_2(\psi) = 2d(d - 2 + \Xi_2(\psi)) = 2d(d - 1 - M_2^{\text{lin}}(\psi)), \quad (71)$$

with  $d = 2^L$ .

## 9 Conclusions

In this work, we have analyzed the Haar-induced probability distributions of measures of non-stabilizerness, specifically the stabilizer Rényi entropies, and uncovered a geometric structure underlying their behavior. Focusing on the single-qubit case, we have shown that the corresponding probability density functions exhibit non-analytic features in the form of logarithmic divergencies, directly analogous to Van Hove singularities in the density of states of condensed matter systems.

By mapping the stabilizer purity to an effective dispersion relation defined on the Bloch sphere, we established a correspondence between the geometry of quantum states and the statistical structure of magic. The singularities emerge at saddle points of this dispersion, where the topology of the intersection between the  $\ell_2$  and  $\ell_{2\alpha}$  spheres changes, and are analytically captured by a logarithmic divergence of the probability density near the critical value  $n_c = 2^{1-\alpha}$ . We derived the exact form of the probability density function for the case  $\alpha = 2$ , confirmed the logarithmic behavior through analytical asymptotics and numerical simulations, and computed the exact mean stabilizer Rényi entropy for one qubit. In practice, the observed divergencies in the magic density imply that, drawing states uniformly at random, most states will have magic similar to that of the  $|H\rangle$ -states – a class of states useful for quantum computation. Extending the analysis to higher-dimensional Hilbert spaces, we showed that such divergencies disappear for  $d \geq 3$ , in accordance with the general theory of densities of states in solids.

Beyond the geometric interpretation of the probability densities, we also identified a direct physical meaning of the stabilizer purity for multiqubit systems: the linear stabilizer entropy quantifies an *incompatibility deficit*, measuring the reduction in non-commutativity with respect to Pauli observables. This connects non-stabilizerness to one of the fundamental aspects of quantum mechanics, the incompatibility of measurements.

Taken together, these results demonstrate that the statistical structure of magic reflects the underlying geometry of quantum state space, and that singularities in its Haar distribution encode transitions between distinct geometric regimes of incompatibility.

## 10 Acknowledgments

D.I. would like to acknowledge the Les Houches summer school 2025 on Exact Solvability and Quantum Information for the opportunity to work on this project while being there as well as B. Jasser for a few comments on an early version of the manuscript. The authors thank Alberto B. P. Junior and coauthors in [80] for the useful exchange of emails. A.H. acknowledges support from the PNRR MUR project PE0000023-NQSTI and the PNRR MUR project CN 00000013-ICSC.

### A Mean value of SRE for one qubit

Here we compute the exact expectation value of the stabilizer 2-Renyi entropy for one qubit

$$\mathbb{E}_\psi[M_2(\psi)] = \int_0^{\ln(\frac{3}{2})} dm m P_{M_2}(m) \quad (72)$$

$$= 2 \int_0^{\ln(\frac{3}{2})} dm m e^{-m} P_{N_2}(2e^{-m} - 1) \quad (73)$$

$$= \int_{1/3}^1 dn \ln\left(\frac{2}{n+1}\right) P_{N_2}(n) \quad (74)$$

$$= \frac{4}{\pi} \int_0^1 dx \ln\left(\frac{2}{n+1}\right) \frac{\theta(A(x) - |B(x) - 4n|)}{\sqrt{A(x)^2 - (B(x) - 4n)^2}} \quad (75)$$

$$= \frac{1}{\pi} \int_0^1 dx \int_{-A(x)}^{A(x)} du \frac{\ln\left(\frac{8}{B(x)-u+4}\right)}{\sqrt{A(x)^2 - u^2}} \quad (76)$$

$$= \ln(8) - \frac{1}{\pi} \int_0^1 dx \int_{-A(x)}^{A(x)} du \frac{\ln(B(x) - u + 4)}{\sqrt{A(x)^2 - u^2}} \quad (77)$$

$$= \ln(8) - \frac{1}{\pi} \int_0^1 dx \int_{-\pi/2}^{\pi/2} d\phi \ln(B(x) - A(x) \sin \phi + 4) \quad (78)$$

$$= \ln(8) - \int_0^1 dx \ln\left(\frac{B(x) + 4 + \sqrt{(B(x) + 4)^2 - A(x)^2}}{2}\right) \quad (79)$$

$$= \int_0^1 dx \ln\left(\frac{16}{7x^4 - 6x^2 + 4\sqrt{3x^8 - 5x^6 + 8x^4 - 5x^2 + 3} + 7}\right) \simeq 0.228921, \quad (80)$$

using the following substitutions  $n = 2e^{-m} - 1$ ,  $u = B(x) - 4n$  and  $u = A(x) \sin \phi$  with  $A(x) = (1 - x^2)^2$  and  $B(x) = 3A(x) + 4x^4$ .

### B Change of variables

The aim of this section is to carry out a detailed calculation for Eq. (29). When  $n \rightarrow n_c$  we have that the PDF for  $N_2$  reads

$$P_{N_\alpha}(n) \propto -\ln|n - n_c|.$$

Hence, given

$$P_{\Xi_\alpha}(\xi) = 2P_{N_\alpha}(2\xi - 1), \quad P_{M_\alpha}(m) = 2(\alpha - 1)e^{(1-\alpha)m} P_{N_\alpha}(2e^{(1-\alpha)m} - 1). \quad (81)$$

we can use the change of variables as follows

$$\lim_{n \rightarrow n_c} P_{\Xi_\alpha}(\xi) = 2 \lim_{n \rightarrow n_c} P_{N_\alpha}(2\xi - 1) = 2c \ln|2\xi - 1 - n_c| = 2c \ln\left|\xi - \frac{1+n_c}{2}\right| + 2c \ln 2. \quad (82)$$

where  $c$  is a proportionality constant. In the case of  $M_2$  we have to consider  $m_c = \frac{1+n_c}{1-\alpha} \ln \frac{1+n_c}{2}$  and  $\delta m = m - m_c$  such as  $|\delta m| \ll 1$ . By considering the argument we have that

$$2e^{(1-\alpha)m} - 1 - n_c = 2e^{(1-\alpha)m_c} (e^{(1-\alpha)\delta m} - 1) = 2e^{(1-\alpha)m_c} (1 - \alpha)\delta m + O(\delta m^2). \quad (83)$$

Thus

$$P_{M_\alpha}(m) \propto -\ln|m - m_c|. \quad (84)$$

### C SRE for qudits

When we deal with qudits instead of qubits we have to extend the notion of the Pauli group to that of the Weyl-Heisenberg group. Consider a Hilbert space  $\mathcal{H}_d$  of dimension  $d$  with the orthonormal computational basis  $\{|k\rangle : k \in \mathbb{Z}_d\}$ , where  $\mathbb{Z}_d = \{0, 1, \dots, d-1\}$  is the ring of integers modulo  $d$ . We define two unitary operators, the *shift* operator  $X$  and the *phase* (or *clock*) operator  $Z$ <sup>2</sup>, by

$$X|k\rangle = |k+1\rangle, \quad Z|k\rangle = \omega^k|k\rangle, \quad (85)$$

where  $\omega = e^{2\pi i/d}$  and all index arithmetic is taken modulo  $d$ . These operators generate the basic algebraic structure of the Weyl-Heisenberg group and satisfy

$$X^d = Z^d = \mathbb{1}, \quad (86)$$

and the fundamental commutation rule

$$X^k Z^\ell = \omega^{-k\ell} Z^\ell X^k, \quad (87)$$

for all  $k, \ell \in \mathbb{Z}_d$ . Given a pair of integers  $\mathbf{a} = (a_1, a_2) \in \mathbb{Z}_d^2$ , we introduce the *displacement operator*

$$D_{\mathbf{a}} = \omega^{-\frac{a_1 a_2}{2}} X^{a_1} Z^{a_2}. \quad (88)$$

The prefactor involving  $\frac{a_1 a_2}{2}$  is understood modulo  $d$ , and when  $d$  is even one must adopt a consistent convention for the ‘‘half-integer’’ exponent. The operators  $\{D_{\mathbf{a}}\}_{\mathbf{a} \in \mathbb{Z}_d^2}$  close under multiplication and obey the relations

$$D_{\mathbf{a}}^\dagger = D_{-\mathbf{a}}, \quad D_{\mathbf{a}} D_{\mathbf{b}} = \omega^{\frac{1}{2}[\mathbf{a}, \mathbf{b}]} D_{\mathbf{a}+\mathbf{b}}, \quad (89)$$

where the symplectic form on the discrete phase space  $\mathbb{Z}_d^2$  is  $[\mathbf{a}, \mathbf{b}] = a_1 b_2 - a_2 b_1$ . These operators form an orthogonal basis with respect to the Hilbert-Schmidt inner product, as expressed by

$$\text{Tr}(D_{\mathbf{a}} D_{\mathbf{b}}^\dagger) = d \delta_{\mathbf{a}, \mathbf{b}}. \quad (90)$$

The full Weyl-Heisenberg group  $\mathcal{W}(d)$  is the set of all products of displacement operators and integer powers of the phase factor  $\omega$ :

$$\mathcal{W}(d) = \{\omega^s D_{\mathbf{a}} : s \in \mathbb{Z}_d, \mathbf{a} \in \mathbb{Z}_d^2\}. \quad (91)$$

It contains  $d^3$  elements, corresponding to the  $d^2$  independent displacements and the additional  $d$  possible global phases. Global scalar phases, however, are physically irrelevant and form a central subgroup

$$\mathcal{Z} = \{\omega^s \mathbb{1} : s \in \mathbb{Z}_d\}. \quad (92)$$

Quotienting by this subgroup gives the *phase-free Weyl-Heisenberg group*

$$\overline{\mathcal{W}}(d) = \mathcal{W}(d)/\mathcal{Z}. \quad (93)$$

This quotient identifies all elements that differ by an overall  $d$ -th root of unity. The resulting group has order  $d^2$  and corresponds to taking only those operators whose representative phases are  $+1$ . We are then ready to find the stabilizer purities in the case of qudits as [114]

$$\Xi_\alpha(|\psi\rangle) = \frac{1}{d} \sum_{\mathbf{a}} |\text{Tr}(D_{\mathbf{a}} \psi)|^{2\alpha}, \quad (94)$$

and the SREs

$$M_\alpha(|\psi\rangle) = \frac{1}{1-\alpha} \log_d \Xi_\alpha(|\psi\rangle). \quad (95)$$

Finally, in this context  $N_\alpha(|\psi\rangle) = d \Xi_\alpha(|\psi\rangle) - 1$ .

### D Coherence

In this section, we derive the PDF of the  $\ell_1$  norm of coherence [117] of one qubit defined as

$$C(\rho) = \sum_{i \neq j} |\langle i | \rho | j \rangle| = 2 |\rho_{0,1}|, \quad (96)$$

<sup>2</sup>In analogy to the Pauli matrices  $X$  and  $Z$

with fixed reference basis  $\{|i\rangle\}$ , which in this case we choose to be the Z basis. Namely, in the case of one qubit pure state

$$|\psi\rangle = \cos \frac{\theta}{2} |0\rangle + e^{i\phi} \sin \frac{\theta}{2} |1\rangle, \quad \theta \in [0, \pi] \text{ and } \phi \in [0, 2\pi], \quad (97)$$

we have

$$C(|\psi\rangle\langle\psi|) = \sin \theta. \quad (98)$$

Hence,

$$P_C(c) = \int_0^{2\pi} \int_0^\pi \frac{\sin \theta d\theta d\phi}{4\pi} \delta(C(\theta) - c) = \frac{1}{2} \int_0^\pi \sin \theta d\theta \delta(C(\theta) - c) \quad (99)$$

$$= \frac{1}{2} \sum_{i=1}^2 \frac{\sin \theta_i}{|\cos \theta_i|} = \frac{c}{\sqrt{1-c^2}}, \quad (100)$$

with  $\sin \theta_i = c$  and  $\cos \theta_i = \pm\sqrt{1-c^2}$ .

### E Incompatibility deficit for multi-qubits case

We have defined the partial incompatibility in Eq. (70) of order  $\alpha \geq 1/2$  as

$$\Gamma_\alpha(\psi) = \sum_{P \in \mathcal{P}_L} \|[\psi, P]\|_{2\alpha}^{2\alpha}, \quad (101)$$

where the Schatten  $2\alpha$ -norm is given by  $\|A\|_{2\alpha}^{2\alpha} = \text{Tr}[(A^\dagger A)^\alpha]$ . Additionally, We recall the following identities, valid for pure states and Pauli operators:

$$\psi^2 = \psi, \quad \psi^\dagger = \psi, \quad P^2 = \mathbb{1}, \quad P^\dagger = P. \quad (102)$$

Using these properties, we can write

$$\|[\psi, P]\|_{2\alpha}^{2\alpha} = \text{Tr}([\psi, P]^\dagger [\psi, P]^\alpha). \quad (103)$$

We now define the positive operator

$$\begin{aligned} W &:= [\psi, P]^\dagger [\psi, P] = (\psi P - P\psi)^\dagger (\psi P - P\psi) \\ &= (P\psi - \psi P)(\psi P - P\psi) \\ &= P\psi^2 P - P\psi P\psi - \psi P\psi P + \psi P^2 \psi \\ &= P\psi P + \psi - (P\psi P\psi + \psi P\psi P). \end{aligned} \quad (104)$$

Writing explicitly  $\psi = |\psi\rangle\langle\psi|$  and defining

$$w_P := \langle\psi|P|\psi\rangle, \quad (105)$$

we obtain

$$W = P\psi P + \psi - w_P(P\psi + \psi P). \quad (106)$$

The operator  $W$  has support only on the two-dimensional subspace spanned by  $\{|\psi\rangle, P|\psi\rangle\}$ . It is easy to show that its nonzero eigenvalues are both  $1 - w_P^2$ ,

$$\begin{aligned} W|\psi\rangle &= \{P\psi P + \psi - w_P(P\psi + \psi P)\}|\psi\rangle \\ &= P|\psi\rangle\langle\psi|P|\psi\rangle + |\psi\rangle - w_P(P|\psi\rangle + w_P|\psi\rangle) \\ &= (1 - w_P^2)|\psi\rangle. \end{aligned} \quad (107)$$

and

$$\begin{aligned} WP|\psi\rangle &= \{P\psi P + \psi - w_P(P\psi + \psi P)\}P|\psi\rangle \\ &= P|\psi\rangle + w_P|\psi\rangle - w_P(w_P P|\psi\rangle + |\psi\rangle) \\ &= (1 - w_P^2)P|\psi\rangle. \end{aligned} \quad (108)$$

All remaining eigenvalues vanish. Indeed, for any vector  $|\chi\rangle$  satisfying

$$\langle\psi|\chi\rangle = 0, \quad \langle\psi|P|\chi\rangle = 0, \quad (109)$$

one finds

$$\begin{aligned} W|\chi\rangle &= P|\psi\rangle\langle\psi|P|\chi\rangle + |\psi\rangle\langle\psi|\chi\rangle - w_P(P|\psi\rangle\langle\psi|\chi\rangle + |\psi\rangle\langle\psi|P|\chi\rangle) \\ &= 0. \end{aligned} \quad (110)$$

Therefore,

$$\text{Tr}[W^\alpha] = 2(1 - w_P^2)^\alpha. \quad (111)$$

Substituting into Eq. (70), for integer values of  $\alpha$  we obtain the following finite sum

$$\Gamma_\alpha(\psi) = 2 \sum_P (1 - w_P^2)^\alpha = 2 \sum_P \sum_{s=0}^{\alpha} \binom{\alpha}{s} (-1)^s w_P^{2s} = 2d \sum_{s=0}^{\alpha} \binom{\alpha}{s} (-1)^s \Xi_s(\psi), \quad (112)$$

where  $\Xi_s(\psi)$  denotes the stabilizer purity of order  $s$ . In particular, for  $\alpha = 2$  we find

$$\Gamma_2(\psi) = 2d(d - 2 + \Xi_2(\psi)). \quad (113)$$

## References

- [1] G. Gour, “Resources of the quantum world,” *arXiv:2402.05474*, 2024.
- [2] E. Chitambar and G. Gour, “Quantum resource theories,” *Review of Modern Physics*, vol. 91, pp. 025001–025001, Apr. 2019.
- [3] G. Gour, *Quantum Resource Theories*. Cambridge University Press, 2025.
- [4] R. Horodecki, P. Horodecki, M. Horodecki, and K. Horodecki, “Quantum entanglement,” *Reviews of Modern Physics*, vol. 81, pp. 865–942–865–942, June 2009.
- [5] H.-Y. Huang, S. Choi, J. R. McClean, and J. Preskill, “The vast world of quantum advantage,” *arXiv:2508.05720*, 2025.
- [6] S. Bravyi and A. Kitaev, “Universal quantum computation with ideal Clifford gates and noisy ancillas,” *Physical Review A*, vol. 71, pp. 022316–022316, Feb. 2005.
- [7] E. T. Campbell and D. E. Browne, “Bound States for Magic State Distillation in Fault-Tolerant Quantum Computation,” *Physical Review Letters*, vol. 104, pp. 030503–030503, Jan. 2010.
- [8] B. Eastin and E. Knill, “Restrictions on transversal encoded quantum gate sets,” *Physical Review Lett.*, vol. 102, p. 110502, Mar 2009.
- [9] X. Turkeshi, “Coherent errors make magic,” *Nature Physics*, vol. 20, no. 11, pp. 1696–1697, 2024.
- [10] D. Gottesman, “The Heisenberg representation of quantum computers,” *arxiv:quant-ph/9807006*, 1998.
- [11] S. Aaronson and D. Gottesman, “Improved simulation of stabilizer circuits,” *Physical Review A*, vol. 70, pp. 052328–052328, Nov. 2004.
- [12] V. Veitch, S. A. H. Mousavian, D. Gottesman, and J. Emerson, “The Resource Theory of Stabilizer Quantum Computation,” *New Journal of Physics*, vol. 16, pp. 013009–013009, Jan. 2014.
- [13] A. Heimendahl, M. Heinrich, and D. Gross, “The axiomatic and the operational approaches to resource theories of magic do not coincide,” *Journal of Mathematical Physics*, vol. 63, Nov. 2022.
- [14] H. Zhu, R. Kueng, M. Grassl, and D. Gross, “The Clifford group fails gracefully to be a unitary 4-design,” *arXiv:1609.08172*, 2016.
- [15] D. Iannotti, G. Esposito, L. Campos Venuti, and A. Hamma, “Entanglement and stabilizer entropies of random bipartite pure quantum states,” *Quantum*, vol. 9, p. 1797, July 2025.
- [16] C. Vairogs and B. Yan, “Extracting randomness from magic quantum states,” *Physical Review Res.*, vol. 7, p. L022069, Jun 2025.
- [17] S. Aditya, A. Summer, P. Sierant, and X. Turkeshi, “Mpemba effects in quantum complexity,” *arXiv:2509.22176*, 2025.
- [18] T. Haug and L. Piroli, “Stabilizer entropies and nonstabilizerness monotones,” *Quantum*, vol. 7, p. 1092, Aug. 2023.

- [19] L. Leone, S. F. Oliviero, A. Hamma, J. Eisert, and L. Bittel, “The non-Clifford cost of random unitaries,” *arXiv:2505.10110*, 2025.
- [20] L. Bittel, J. Eisert, L. Leone, A. A. Mele, and S. F. Oliviero, “A complete theory of the Clifford commutant,” *arXiv:2504.12263*, 2025.
- [21] Z.-Y. Hou, C. Cao, and Z.-C. Yang, “Stabilizer entanglement as a magic highway,” *arXiv preprint arXiv:2503.20873*, 2025.
- [22] A. Scocco, W.-K. Mok, L. Aolita, M. Collura, and T. Haug, “Rise and fall of nonstabilizerness via random measurements,” *arXiv:2507.11619*, 2025.
- [23] B. Magni, A. Christopoulos, A. De Luca, and X. Turkeshi, “Anticoncentration in Clifford circuits and beyond: From random tensor networks to pseudomagic states,” *Physical Review X*, vol. 15, no. 3, p. 031071, 2025.
- [24] B. Magni and X. Turkeshi, “Quantum complexity and chaos in many-qudit doped Clifford circuits,” *arXiv:2506.02127*, 2025.
- [25] V. Mittal and Y.-P. Huang, “Quantum magic in discrete-time quantum walk,” *arXiv:2506.17783*, 2025.
- [26] N. D. Varikuti, S. Bandyopadhyay, and P. Hauke, “Impact of Clifford operations on non-stabilizing power and quantum chaos,” *arXiv:2505.14793*, 2025.
- [27] A. Paviglianiti, *Entanglement and Quantum Complexity in Monitored Quantum Many-Body Systems*. PhD thesis, SISSA, Trieste, 2025.
- [28] H. Lóio, G. Lami, L. Leone, M. McGinley, X. Turkeshi, and J. De Nardis, “Quantum state designs via magic teleportation,” *arXiv:2510.13950*, 2025.
- [29] B. Magni, A. Christopoulos, A. De Luca, and X. Turkeshi, “Anticoncentration in Clifford circuits and beyond: From random tensor networks to pseudomagic states,” *Physical Review X*, vol. 15, p. 031071, Sep 2025.
- [30] N. D. Varikuti, S. Bandyopadhyay, and P. Hauke, “Impact of Clifford operations on non-stabilizing power and quantum chaos,” *arXiv:2505.14793*, 2025.
- [31] Y. Zhang and Y. Gu, “Quantum magic dynamics in random circuits,” *arXiv:2410.21128*, 2024.
- [32] S. F. E. Oliviero, L. Leone, and A. Hamma, “Magic-state resource theory for the ground state of the transverse-field Ising model,” *Physical Review A*, vol. 106, p. 042426, Oct. 2022. Publisher: American Physical Society.
- [33] T. Haug and L. Piroli, “Quantifying nonstabilizerness of matrix product states,” *Physical Review B*, vol. 107, p. 035148, Jan. 2023. Publisher: American Physical Society.
- [34] G. Passarelli, R. Fazio, and P. Lucignano, “Nonstabilizerness of permutationally invariant systems,” *Physical Review A*, vol. 110, p. 022436, Aug. 2024. Publisher: American Physical Society.
- [35] G. Passarelli, P. Lucignano, D. Rossini, and A. Russomanno, “Chaos and magic in the dissipative quantum kicked top,” *Quantum*, vol. 9, p. 1653, Mar. 2025. Publisher: Verein zur Förderung des Open Access Publizierens in den Quantenwissenschaften.
- [36] D. Rattacaso, L. Leone, S. F. E. Oliviero, and A. Hamma, “Stabilizer entropy dynamics after a quantum quench,” *Physical Review A*, vol. 108, p. 042407, Oct. 2023. Publisher: American Physical Society.
- [37] E. Tirrito, X. Turkeshi, and P. Sierant, “Anticoncentration and magic spreading under ergodic quantum dynamics,” *arXiv:2412.10229*, 2024.
- [38] E. Tirrito, P. S. Tarabunga, D. S. Bhakuni, M. Dalmonte, P. Sierant, and X. Turkeshi, “Universal spreading of nonstabilizerness and quantum transport,” *arXiv:2506.12133*, 2025.
- [39] E. Tirrito, L. Lumia, A. Paviglianiti, G. Lami, A. Silva, X. Turkeshi, and M. Collura, “Magic phase transitions in monitored gaussian fermions,” *arXiv:2507.07179*, 2025.
- [40] A. Russomanno, G. Passarelli, D. Rossini, and P. Lucignano, “Efficient evaluation of the nonstabilizerness in unitary and monitored quantum many-body systems,” *arXiv:2502.01431*, 2025.

- [41] G. Passarelli, A. Russomanno, and P. Lucignano, “Nonstabilizerness of a boundary time crystal,” *Physical Review A*, vol. 111, p. 062417, June 2025. Publisher: American Physical Society.
- [42] D. Sticlet, B. Dóra, D. Szombathy, G. Zaránd, and C. P. Moca, “Non-stabilizerness in open xxz spin chains: Universal scaling and dynamics,” *arXiv:2504.11139*, 2025.
- [43] M. Viscardi, M. Dalmonte, A. Hamma, and E. Tirrito, “Interplay of entanglement structures and stabilizer entropy in spin models,” *arXiv:2503.08620*, 2025.
- [44] B. Jasser, J. Odavić, and A. Hamma, “Stabilizer Entropy and entanglement complexity in the Sachdev-Ye-Kitaev model,” *Physical Review B*, Sept. 2025. Publisher: American Physical Society.
- [45] M. Collura, J. De Nardis, V. Alba, and G. Lami, “The quantum magic of fermionic gaussian states,” *arXiv:2412.05367*, 2024.
- [46] P. R. N. Falcão, P. S. Tarabunga, M. Frau, E. Tirrito, J. Zakrzewski, and M. Dalmonte, “Nonstabilizerness in U(1) lattice gauge theory,” *Physical Review B*, vol. 111, p. L081102, Feb. 2025. Publisher: American Physical Society.
- [47] F. Brökemeier, S. M. Hengstenberg, J. W. T. Keeble, C. E. P. Robin, F. Rocco, and M. J. Savage, “Quantum magic and multipartite entanglement in the structure of nuclei,” *Physical Review C*, vol. 111, p. 034317, Mar. 2025. Publisher: American Physical Society.
- [48] P. S. Tarabunga and T. Haug, “Efficient mutual magic and magic capacity with matrix product states,” *SciPost Phys.*, vol. 19, p. 085, 2025.
- [49] M. Frau, P. S. Tarabunga, M. Collura, M. Dalmonte, and E. Tirrito, “Nonstabilizerness versus entanglement in matrix product states,” *Physical Review B*, vol. 110, p. 045101, Jul 2024.
- [50] S. Sarkar, C. Mukhopadhyay, and A. Bayat, “Characterization of an operational quantum resource in a critical many-body system,” *New Journal of Physics*, vol. 22, p. 083077, Aug. 2020.
- [51] Z.-W. Liu and A. Winter, “Many-body quantum magic,” *PRX Quantum*, vol. 3, May 2022.
- [52] X. Turkeshi, A. Dymarsky, and P. Sierant, “Pauli spectrum and nonstabilizerness of typical quantum many-body states,” *Physical Review B*, vol. 111, p. 054301, Feb 2025.
- [53] P. Zhang, S. Zhou, and N. Sun, “Stabilizer Rényi Entropy entropy and its transition in the coupled Sachdev-Ye-Kitaev model,” *arXiv:2509.17417*, 2025.
- [54] C. Moca, D. Sticlet, B. Dóra, A. Valli, D. Szombathy, and G. Zaránd, “Non-stabilizerness generation in a multi-particle quantum walk,” *arXiv:2504.19750*, 2025.
- [55] S. Bera and M. Schirò, “Non-stabilizerness of Sachdev-Ye-Kitaev model,” *arXiv:2502.01582*, 2025.
- [56] D. A. Korbany, M. J. Gullans, and L. Piroli, “Long-range nonstabilizerness and phases of matter,” *Physical Review Letters*, vol. 135, Oct. 2025.
- [57] T. Haug and L. Piroli, “Quantifying nonstabilizerness of matrix product states,” *Physical Review B*, vol. 107, p. 035148, Jan 2023.
- [58] P. S. Tarabunga, E. Tirrito, M. C. Bañuls, and M. Dalmonte, “Nonstabilizerness via matrix product states in the Pauli basis,” *Physical Review Lett.*, vol. 133, p. 010601, Jul 2024.
- [59] D. Sticlet, B. Dóra, D. Szombathy, G. Zaránd, and C. Moca, “Non-stabilizerness in open xxz spin chains: Universal scaling and dynamics,” *arXiv:2504.11139*, 2025.
- [60] B. Dóra and C. Moca, “Momentum space nonstabilizerness for the transverse field quantum ising model,” *Physical Review B*, vol. 112, p. 125427, Sep 2025.
- [61] C. P. Moca, D. Sticlet, and B. Dóra, “Non-stabilizerness as a diagnostic of criticality and exceptional points in non-hermitian spin chains,” 2025.
- [62] M. Sarkis and A. Tkatchenko, “Are molecules magical? non-stabilizerness in molecular bonding,” *arXiv:2504.06673*, 2025.
- [63] M. J. Savage, “Quantum simulations of fundamental physics,” *arXiv:2503.23233*, 2025.

- [64] C. E. P. Robin and M. J. Savage, “Quantum complexity fluctuations from nuclear and hypernuclear forces,” *Physical Review C*, vol. 112, Oct. 2025.
- [65] G. Busoni, J. Gargalionis, E. N. Wallace, and M. J. White, “Emergent symmetry in a two-higgs-doublet model from quantum information and nonstabilizerness,” *Physical Review D*, vol. 112, Aug. 2025.
- [66] M. Illa, M. J. Savage, and X. Yao, “Dynamical local tadpole-improvement in quantum simulations of gauge theories,” *arXiv:2504.21575*, 2025.
- [67] C. D. White and M. J. White, “Magic states of top quarks,” *Physical Review D*, vol. 110, p. 116016, Dec. 2024. Publisher: American Physical Society.
- [68] R. Aoude, H. Banks, C. D. White, and M. J. White, “Probing new physics in the top sector using quantum information,” *arXiv:2505.12522*, 2025.
- [69] S. Cepollaro, S. Cusumano, A. Hamma, G. L. Giudice, and J. Odavic, “Harvesting stabilizer entropy and non-locality from a quantum field,” *Physical Review D*, 2024.
- [70] Q. Liu, I. Low, and Z. Yin, “Quantum magic in quantum electrodynamics,” *arXiv:2503.03098*, 2025.
- [71] G. Esposito, S. Cepollaro, L. Cappiello, and A. Hamma, “Magic of discrete lattice gauge theories,” *International Journal of Geometric Methods in Modern Physics*, vol. 22, no. 6, pp. 2550003–352, 2025.
- [72] M. Hoshino, M. Oshikawa, and Y. Ashida, “Stabilizer Rényi Entropy entropy and conformal field theory,” *arXiv:2503.13599*, 2025.
- [73] M. Frau, P. S. Tarabunga, M. Collura, E. Tirrito, and M. Dalmonte, “Stabilizer disentangling of conformal field theories,” *SciPost Physics*, vol. 18, p. 165, May 2025.
- [74] M. Hoshino and Y. Ashida, “Stabilizer Rényi Entropy entropy encodes fusion rules of topological defects and boundaries,” *arXiv:2507.10656*, 2025.
- [75] J. R. Fliss, “Knots, links, and long-range magic,” *Journal of High Energy Physics*, vol. 2021, Apr. 2021.
- [76] M. Howard, E. Brennan, and J. Vala, “Quantum contextuality with stabilizer states,” *Entropy*, vol. 15, p. 2340–2362, June 2013.
- [77] R. A. Macedo, P. Andriolo, S. Zamora, D. Poderini, and R. Chaves, “Witnessing magic with bell inequalities,” *arXiv:2503.18734*, 2025.
- [78] L. Leone, S. F. E. Oliviero, and A. Hamma, “Stabilizer Rényi Entropy,” *Physical Review Letters*, vol. 128, pp. 050402–050402, Feb. 2022.
- [79] D. Szombathy, A. Valli, C. Moca, J. Asbóth, L. Farkas, T. Rakovszky, and G. Zaránd, “Spectral properties versus magic generation in  $T$ -doped random Clifford circuits,” *Physical Review Letters*, **7**, 043080 (2025).
- [80] A. B. P. Junior, S. Zamora, R. A. Macêdo, T. S. Sarubi, J. M. Varela, G. W. C. Rocha, D. A. Moreira, and R. Chaves, “Geometric analysis of the stabilizer polytope for few-qubit systems,” 2025.
- [81] L. Leone, S. F. E. Oliviero, and A. Hamma, “Nonstabilizerness determining the hardness of direct fidelity estimation,” *Physical Review A*, vol. 107, p. 022429, Feb 2023.
- [82] M. A. Nielsen and I. L. Chuang, *Quantum Computation and Quantum Information: 10th Anniversary Edition*. Cambridge University Press, 2010.
- [83] J. Watrous, “Understanding quantum information and computation,” *arXiv:2507.11536*, 2025.
- [84] V. Veitch, S. A. Hamed Mousavian, D. Gottesman, and J. Emerson, “The resource theory of stabilizer quantum computation,” *New Journal of Physics*, vol. 16, p. 013009, Jan. 2014.
- [85] M. Howard and E. Campbell, “Application of a Resource Theory for Magic States to Fault-Tolerant Quantum Computing,” *Physical Review Letters*, vol. 118, pp. 090501–090501, Mar. 2017.

- [86] H. Zhu, R. Kueng, M. Grassl, and D. Gross, “The Clifford group fails gracefully to be a unitary 4-design,” *arXiv:1609.08172*, 2016.
- [87] L. Bittel and L. Leone, “Operational interpretation of the stabilizer entropy,” *arXiv:2507.22883*, 2025.
- [88] L. Leone and L. Bittel, “Stabilizer entropies are monotones for magic-state resource theory,” *Physical Review A*, vol. 110, p. L040403, Oct 2024.
- [89] S. F. E. Oliviero, L. Leone, A. Hamma, and S. Lloyd, “Measuring magic on a quantum processor,” *npj Quantum Inf*, vol. 8, pp. 1–8, Dec. 2022.
- [90] T. Haug, S. Lee, and M. Kim, “Efficient quantum algorithms for stabilizer entropies,” *Physical Review Letters*, vol. 132, June 2024.
- [91] T. Haug and M. Kim, “Scalable measures of magic resource for quantum computers,” *PRX Quantum*, vol. 4, p. 010301, Jan 2023.
- [92] R. J. Garcia, G. Bhole, K. Bu, L. Chen, H. Arthanari, and A. Jaffe, “Hardness of measuring magic resource,” *Physical Review Research*, vol. 7, no. 3, p. 033271, 2025.
- [93] B. Stratton, “An algorithm for estimating  $\alpha$ -stabilizer rényi entropies via purity,” *arXiv:2507.02540*, 2025.
- [94] P. Niroula, C. D. White, Q. Wang, S. Johri, D. Zhu, C. Monroe, C. Noel, and M. J. Gullans, “Phase transition in magic with random quantum circuits,” *Nature Physics*, vol. 20, p. 1786–1792, Sept. 2024.
- [95] M. Bejan, C. McLauchlan, and B. Béri, “Dynamical magic transitions in monitored Clifford+ $t$  circuits,” *PRX Quantum*, vol. 5, p. 030332, Aug 2024.
- [96] G. E. Fux, E. Tirrito, M. Dalmonte, and R. Fazio, “Entanglement – nonstabilizerness separation in hybrid quantum circuits,” *Physical Review Research*, vol. 6, Oct. 2024.
- [97] L. Leone, S. F. E. Oliviero, G. Esposito, and A. Hamma, “Phase transition in stabilizer entropy and efficient purity estimation,” *Physical Review A*, vol. 109, Mar. 2024.
- [98] X. Turkeshi, M. Schirò, and P. Sierant, “Measuring nonstabilizerness via multifractal flatness,” *Physical Review A*, vol. 108, p. 042408, Oct 2023.
- [99] C. Castellani, “Multifractal wavefunction at the localization threshold,” in *Fluctuations and Stochastic Phenomena in Condensed Matter: Proceedings of the Sitges Conference on Statistical Mechanics Sitges, Barcelona/Spain, May 26–30, 1986*, pp. 315–332, Springer, 2005.
- [100] J.-M. Stéphan, S. Furukawa, G. Misguich, and V. Pasquier, “Shannon and entanglement entropies of one- and two-dimensional critical wave functions,” *Physical Review B*, vol. 80, p. 184421, Nov 2009.
- [101] L. Leone, S. F. E. Oliviero, Y. Zhou, and A. Hamma, “Quantum chaos is quantum,” *Quantum*, vol. 5, p. 453, May 2021.
- [102] R. J. Garcia, K. Bu, and A. Jaffe, “Resource theory of quantum scrambling,” *Proceedings of the National Academy of Sciences*, vol. 120, Apr. 2023.
- [103] I. Bengtsson and K. Życzkowski, *Geometry of Quantum States: An Introduction to Quantum Entanglement*. Cambridge University Press, 2006.
- [104] W. K. Wootters, “Random quantum states,” *Foundations of Physics*, vol. 20, no. 11, pp. 1365–1378, 1990.
- [105] A. A. Mele, “Introduction to haar measure tools in quantum information: A beginner’s tutorial,” *Quantum*, vol. 8, p. 1340, May 2024.
- [106] B. Collins and P. Śniady, “Integration with respect to the haar measure on unitary, orthogonal and symplectic group,” *Communications in Mathematical Physics*, vol. 264, no. 3, pp. 773–795, 2006.
- [107] J. Watrous, *The theory of quantum information*. Cambridge university press, 2018.
- [108] B. Collins and I. Nechita, “Random matrix techniques in quantum information theory,” *Journal of Mathematical Physics*, vol. 57, Dec. 2015.

- [109] O. Giraud, “Purity distribution for bipartite random pure states,” *Journal of Physics A: Mathematical and Theoretical*, vol. 40, no. 49, p. F1053, 2007.
- [110] N. F. Q. Yuan, “Classification of critical points in energy bands based on topology, scaling, and symmetry,” *Physical Review B*, vol. 101, no. 12, 2020.
- [111] M. Heinrich and D. Gross, “Robustness of magic and symmetries of the stabiliser polytope,” *Quantum*, vol. 3, p. 132, Apr. 2019.
- [112] R. S. Palais, “The principle of symmetric criticality,” *Communications in Mathematical Physics*, vol. 69, no. 1, pp. 19–30, 1979.
- [113] I. Gradshteyn, I. Ryzhik, and R. H. Romer, *Tables of integrals, series, and products*. American Association of Physics Teachers, 1988.
- [114] Y. Wang and Y. Li, “Stabilizer Rényi entropy on qudits,” *Quant. Inf. Proc.*, vol. 22, no. 12, p. 444, 2023.
- [115] V. Kendon, K. Nemoto, and W. Munro, “Typical entanglement in multiple-qubit systems,” *Journal of Modern Optics*, vol. 49, p. 1709–1716, Aug. 2002.
- [116] L. Campos Venuti and P. Zanardi, “Probability density of quantum expectation values,” *Physics Letters A*, vol. 377, pp. 1854–1861, Oct. 2013.
- [117] T. Baumgratz, M. Cramer, and M. B. Plenio, “Quantifying Coherence,” *Physical Review Lett.*, vol. 113, p. 140401, Sept. 2014.
- [118] A. B. P. Junior 2025. Private communication.
- [119] J. J. Sakurai and J. Napolitano, *Modern quantum mechanics*. Cambridge University Press, 2020.